JOURNAL OF MATERIALS SCIENCE 30 (1995) 3625–3632

Yield stress behaviour of metal injection moulding suspensions at elevated temperatures

M. L. FOONG, K. C. TAM*, N. H. LOH
School of Mechanical and Production Engineering, Nanyang Technological University, Nanyang Avenue, Singapore 2263

Yield behaviour of metal injection moulding (MIM) feedstocks was studied using a cone and plate controlled stress rheometer. Four feedstocks consisting of 58 vol% carbonyl iron (with 2 wt% nickel) in different ethylene vinyl acetate (EVA):beeswax ratio binder systems were studied at six temperatures ranging from 130 to 180 °C. The yield stress was found by extrapolating to zero shear rate of the measured data obtained using a controlled stress rheometer over low shear rate regime. The yield stress, τ_y, was found to increase with decreasing temperature. An Arrhenius equation was used to relate the dependence of yield stress on temperature and the corresponding activation energy for yield, E_y, can be determined. For a given temperature, feedstocks with higher EVA content exhibited higher τ_y and E_y. Moreover, the effect of temperature on yield stress was found to be greater for feedstocks with higher EVA content.

1. Introduction

Metal injection moulding (MIM) is a relatively new process that combines plastic and conventional powder metallurgy technology. A schematic representation of this process is summarized in Fig. 1. It is best suited for production of small complex parts. Its main advantage lies in its ability to produce parts to net shape without the need for expensive secondary operations. Hence, it is very attractive for hard metals, cermets or even metal matrix composites.

The key to MIM is incorporating a transport medium into a metal power. The medium, or binder, serves to carry the powder and allow flow and packing of the powder in the mould cavity. The binder is basically a blend of either a thermoplastic or thermoset with waxes and additives. There are various types of binder formulations being developed, many of which are covered by patents [1–10].

To minimize dimensional shrinkage and distortions after debinding, the concentration of powder in a feedstock is made very high, usually in the range of 50–80% by volume. During moulding, the feedstock is essentially a highly concentrated suspension caused to flow and fill the mould cavity by the action of pressure and temperature. For successful moulding, it is important to understand and be able to predict the flow behaviour of the feedstock within the mould cavity. It has been reported that during injection moulding, the shear rates vary typically from 10^2 to 10^5 s^{-1} [11, 12]. However, it should be noted that conditions, including temperature, pressure, flow velocity, shear stress and shear rates of the feedstock, vary from location to location. Conditions encountered by the feedstock in the nozzle is different from that in runners, gates and within the mould cavity. Depending on the complexity of the mould geometry, conditions within the mould cavity could vary as well. Hence, in order to optimize the moulding process to achieve good moulded parts, it is important to study and obtain the full rheological characterization of the feedstock. This notion was supported and described by German [13].

Yield behaviour is one phenomenon reportedly exhibited by MIM feedstocks at low shear rates and low shear stress conditions. In other words, even at temperatures above its melting point, the feedstock will flow only after a critical minimum shear stress (yield stress) is attained. When the shear stress is below the yield stress, the fluid behaves as a solid and does not flow at all. The existence of yield behaviour has been reported by investigators in the field of powder injection moulding, such as Edirisinghe and Evans [12], German [14] and Rhee [15]. However, to date, no comprehensive study of this behaviour has been reported. The understanding of the yield behaviour of the feedstock is important in optimizing the MIM process. In injection moulding, the presence of a yield stress would influence the flow behaviour of the feedstock into the mould, as well as within the mould cavity. Hence, a proper understanding of this phenomenon would serve as a guide to determine the processing parameters, such as injection speed, moulding temperature and pressure. It would also provide valuable information for the design of moulds to ensure progressive filling and prevent premature gate sealing. In debinding, the yield stress of the feedstock is necessary to support the shape of the compact and prevent

* To whom correspondence should be addressed.

0022–2461 © *1995 Chapman & Hall*

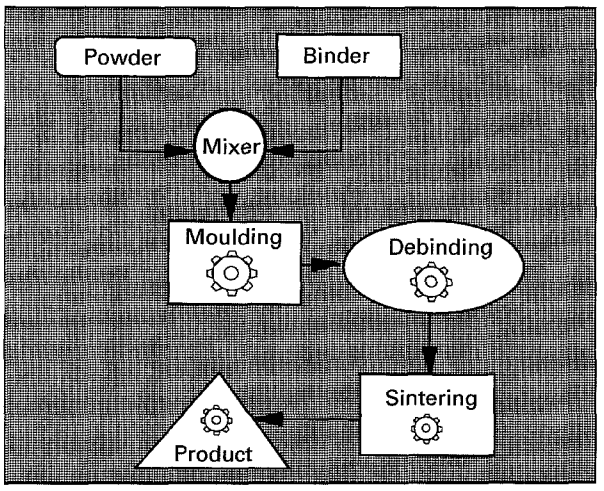

Figure 1 The metal injection moulding process.

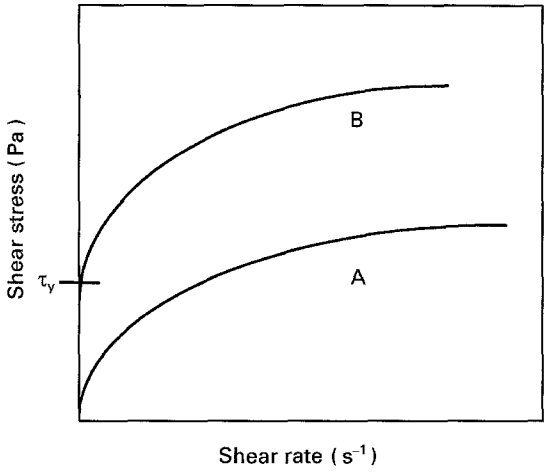

Figure 2 Yield stress of viscoplastic fluid.

slumping under its own weight. A good understanding of the effect of temperature on yield stress would also serve as a guide to designing a good debinding schedule.

This paper attempts to study the low shear behaviour of a feedstock using a cone and plate controlled stress rheometer. The paper aims to confirm the existence of yield stress in MIM feedstocks and to study the effects of temperature and binder formulation on the yield stress.

1.1. Yield stress

A yield stress of a fluid can be defined as the limiting shear stress that has to be exceeded to initiate a shear flow [16]. A fluid that exhibits such a yield stress is termed viscoplastic [17]. When an applied stress is less than a particular stress (yield stress), the fluid will not flow, but deforms plastically like a solid with a certain strain recovery upon the removal of the stress. When the stress exceeds the yield stress, the fluid will flow like a viscous fluid with a finite viscosity [17]. This concept is best illustrated by a plot of shear stress versus shear rate, as shown in Fig. 2. The flow behaviour of a normal viscous fluid (for example, polymer melt) would follow curve A. The curve would begin at the origin, indicating zero shear stress at zero shear rate. A viscoplastic fluid, on the other hand, would only start to flow after the shear stress has exceeded the yield stress, τ_y, as shown by curve B.

Yield stress fluids can be found in a diversity of fields, such as biomedical, food processing and engineering materials. Important examples include concentrated suspensions, pastes, emulsions, gels, paints, blood and other body fluids.

A great amount of work has been done on yield stress in concentrated suspensions [16–31]. However, much of the mechanics of the yield behaviour in suspensions remains unanswered. There are even differing opinions on the existence of a true yield stress in fluids, i.e. whether it is a real material property or just a virtual observation dependent on the time scale of the measuring techniques [18–20].

Measuring yield stress of concentrated suspensions can be carried out using various rheological techniques that can be broadly classified under two categories: the controlled rate rheometry and the controlled stress rheometry. A controlled rate rheometer deforms a specimen at a constant shear rate and measures the shear stress. On the other hand, a controlled stress rheometer imposes a constant shear stress on a specimen and then measures the corresponding strain. The latter approach involves a more sophisticated control system and this has only been introduced in the last ten years. These techniques can be further classified as direct (or static) or indirect methods (or dynamic). The indirect determination of yield stress involves the extrapolation of experimental shear stress–shear rate data to obtain a yield stress, which is the shear stress at zero shear rate. This is illustrated in Fig.3. It is evident that the choice of the model or methods yields differing values of yield stress.

The direct method involves measuring the yield stress directly and is independent of the shear stress–shear rate curves. However, the accuracy depends on the sensitivity of the equipment and the skills of the investigators. Reviews on the various measurement techniques of yield stress fluids have been described by Nguyen and Boger [17] and Kee and Durning [20]. Some of the techniques discussed include the vane method developed by Nguyen and Boger [21, 22], parallel disc rheometry [23, 24], parallel plate [25], cone and plate rheometry [26, 27], falling ball method [18] and the inclined plane method [17]. Of course, there is no single best method to measure yield stress of fluids. Every method has its advantages, as well as its limitations, as highlighted in the reviews [17,28]. Therefore, the choice of method would depend very much on the accuracy required and the intended application of the results. Moreover, the limitations of a chosen method must be taken into account and steps taken to either reduce or correct for any errors that might arise due to these limitations.

1.2. Rheological models for fluids exhibiting yield stress

To date, there are various models developed to describe the flow behaviour of a fluid exhibiting yield

stress. The three most common models used are listed below

The Bingham model [29]

$$\tau = \tau_y + \eta_p \dot{\gamma}, \qquad \tau \geqslant \tau_y \tag{1}$$

The Herschel–Bulkley model [30]

$$\tau = \tau_y + k(\dot{\gamma})^m, \qquad \tau \geqslant \tau_y \tag{2}$$

where k and m are constants.

The Casson model [31]

$$\tau^{1/2} = \tau_y^{1/2} + (\eta_\infty \dot{\gamma})^{1/2}, \qquad \tau \geqslant \tau_y \tag{3}$$

2. Experimental procedure

2.1. Materials

The powder used in the feedstock is carbonyl iron (supplied by BASF) with 2 wt % nickel powder added. The characteristics of the powders are listed in Table I.

Carbonyl iron powder is commonly used in metal injection moulding. This powder is produced by a process known as carbonyl decomposition. This process is capable of achieving very small, spherical shaped powders with smooth surface characteristics. Such properties enable the powder to have good packing characteristics and is ideal for MIM work. Nickel powder is normally added to improve properties of the final sintered products.

The binder used is a blend of ethylene vinyl acetate (EVA) grade 460 copolymer and beeswax. The EVA (supplied by Dupont) has a 17.5–18.5% vinyl acetate content and a melt index of 2.2–2.8 dg min^{-1}. The relevant properties of the binder components are listed in Table II.

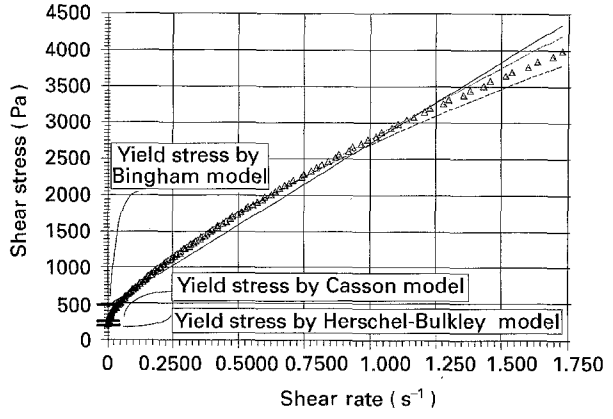

Figure 3 Determination of yield stress of feedstock No. 3 at 170 °C by different mathematical models: (△) experimental data, (—) Bingham model, (----) Casson model, (–––) Herschel–Bulkley model.

EVA is a copolymer manufactured by polymerization of ethylene and vinyl acetate. The polymerization process causes the formation of acetoxy side chains that are polar in nature. Due to the polar side chains, EVA has been reported to have good adhesion between the metal powder and the binder that helps to improve the moulded body's strength and also to reduce powder–binder separation [15, 32–34].

Wax, with a lower molecular weight and shorter molecular chain, is usually added to a binder to reduce the overall feedstock viscosity. At 170 °C, the beeswax used in this experiment has rheological properties near to that of water. Moreover, wax, which has a lower burn-off temperature compared to most polymers, enables progressive debinding during the binder removal process.

2.2. Feedstock formulations

Fig. 4 shows a scanning electron micrograph of a cut surface of feedstock No. 1. As indicated on the figure, the carbonyl iron powder and nickel powder particles are spherical in shape. The grass-like white structures are the EVA copolymers being torn during cutting of the specimen.

Four types of feedstock formulations were used in the experiments. All the feedstocks had the same powder loading (58 vol %), but the binder contents were different. The binder formulations are listed in Table III.

The feedstocks were mixed separately using a Haake–Rheocord torque mixer with a roller rotor attached. The mixing temperature was set at 160–170 °C, which is about 1.5 times the melting temperature of EVA 460. The torque required by the mixer was monitored during mixing. Homogeneity was considered to be achieved once a constant mixing torque was obtained. A typical torque–time curve of mixing is shown in Fig. 5. The mixing was then continued for a further 15 min before stopping and removing the feedstock from the mixer.

2.3. Rheological measurements

The Carri-Med CSL 500 controlled stress rheometer was used for the yield stress and rheological measurements. The CSL500 is equipped with a microprocessor controlled induction motor drive coupled with an air bearing and a high resolution digital optical displacement encoder. The drive is capable of delivering 2×10^{-6} to 5×10^{-2} Nm torque with a resolution of 1×10^{-7} Nm steps. The angular velocity resolution is 1×10^{-4} rad s^{-1} [35].

TABLE I Properties of powders used in feedstocks

Powder	Particle shape	Particle size (μm)	Pycnometer density (g cm^{-3})	Apparent density (g cm^{-3})	Relative surface area (m^2 g^{-1})
Carbonyl iron	Spherical	4–5	7.65	4.1	1.90
Nickel	Spherical	7–10	8.84	3.2	0.15

TABLE II Properties of EVA grade 460 and beeswax

Binder component	Melting temperature (°C)	Softening temperature (°C)	Pycnometer density (g cm^{-3})
EVA 460	94.32	83.99	0.9362
Beeswax	62.53	58.18	0.9552

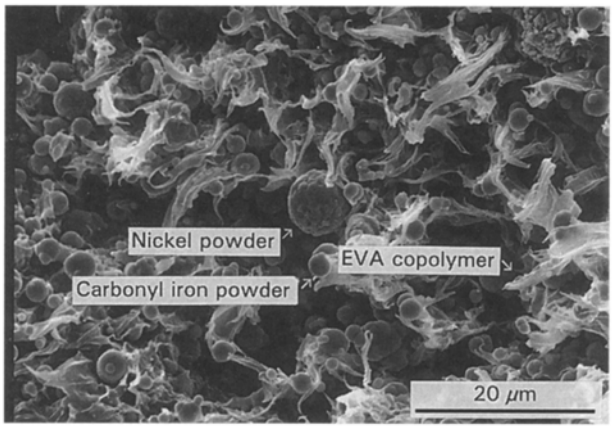

Figure 4 Scanning electron micrograph of a cut surface of feedstock No. 1.

TABLE III Feedstock formulations

Feedstocks	No. 1	No. 2	No. 3	No. 4
EVA 460 (wt.%)	30	40	60	70
Beeswax (wt.%)	70	60	40	30
Powder (vol.%)	58	58	58	58

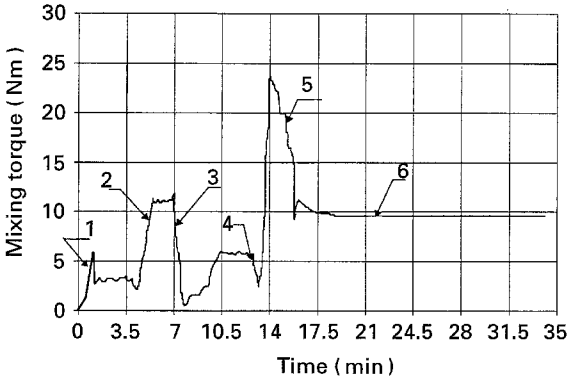

Figure 5 A typical mixing curve for the feedstocks: addition of (1) EVA, (2) half amount metal powder, (3) half amount beeswax, (4) remaining metal powder, (5) remaining beeswax, (6) steady state torque.

A stainless steel cone and plate geometry is used for the experiments. The cone is a 2 cm diameter, angle 2°, truncated cone with a gap set at 51 μm from the plate. The surfaces are smooth and ungrooved. During a test, the plate is kept stationary while the shearing torque is provided by the cone. A steady stream of nitrogen gas is introduced to provide an inert environment throughout the test. An induction heating system (extended temperature module) is provided for high temperature testing environments of up to 400 °C. Temperature control accuracy is ± 0.5 °C. The rheometer is equipped with an innovative auto-gap set system to correct for the thermal expansion of the cone and plate when the tests are performed at different temperatures. This means that the gap between the cone and plate is always set at 51 μm regardless of any temperature variation.

3. Results and discussion

3.1. Yield stress determination

Samples of the feedstocks were tested using a controlled stress cone and plate rheometer. The shear stress was controlled and varied while the corresponding strain was measured. During the test, the shear stress level was first set at a level at which no flow was observed. The stress was then gradually increased in finite steps and the corresponding shear rate was monitored. To observe the flow behaviour, a plot of shear stress versus shear rate can be obtained from the data. Fig.6 shows such a plot for feedstock No. 3 at various temperatures.

It can be observed that the flow curves do not start at the origin but at some finite level of shear stress before any shear rate can be detected. This indicates the existence of a static yield stress that occurs at the intersection of the flow curve and the shear stress axis. However, in reality it is not possible to obtain this "shear stress at zero shear rate" experimentally, without involving any form of extrapolation. This is because the lowest shear rate level detectable by a rheometer upon yielding of the specimen, is finite, no matter how small this value is. Hence, a method of determining the yield stress using a controlled stress rheometer at elevated temperature is proposed.

With the Carri–Med CSL500 controlled stress rheometer, the yield stress can be obtained by direct measurement. Instead of shear rate, the shear stress is varied. Measurement of strain can be carried out from low to high stress levels. The control system will increase the shear stress level in steps and the direct measured yield stress corresponds to the stress level

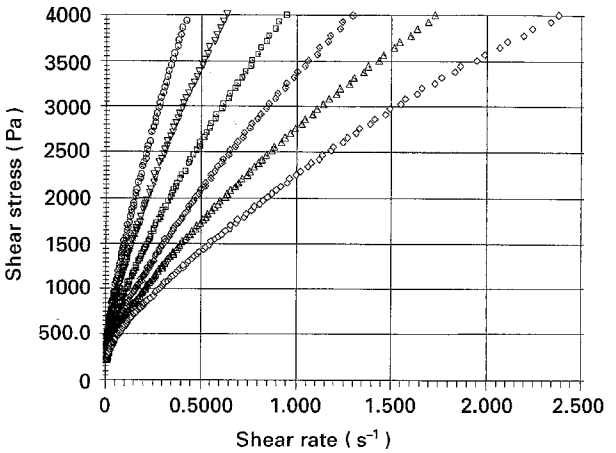

Figure 6 Shear stress versus shear rate plot for feedstock No. 3 at various temperatures: (○) 130, (▽) 140, (□) 150, (◇) 160, (△) 170 and (◇) 180 °C.

recorded at which flow is detected. For the CSL500, this corresponded to the system's resolution of angular velocity 0.0001 rad s^{-1}. However for highly filled suspensions, some fluctuations in the stress data are observed at low deformation. A more accurate method proposed here is to conduct the test over a stress level at which flow is first detected. The data obtained within this range are then fitted with a straight line by the least square method and subsequently extrapolated to intercept the vertical shear stress axis. The yield stress value, τ_y, is obtained from the intersection of the extrapolated line and the axis. This is illustrated in Fig. 7 in which the yield stresses of feedstock No. 3 are estimated at 130, 150 and 170 °C.

For consistency, data range for shear rates 0.03 s^{-1} and below is analysed using the proposed method. It is believed that this method would yield a more accurate τ_y value with the given experimental set up and reflect a value closer to the actual static yield stress of the material. For comparison, the yield stress values of feedstock No. 3 were obtained using direct measurement, as well as calculated from fitting the full range of rheological data (Fig. 6) to the Bingham, Casson and Herschel–Bulkley models. Fitting of the data was achieved by means of linearization and least square method. The yield stress values calculated from the models were chosen so as to give the best fit to the overall data. The yield stress values obtained are listed in Table IV.

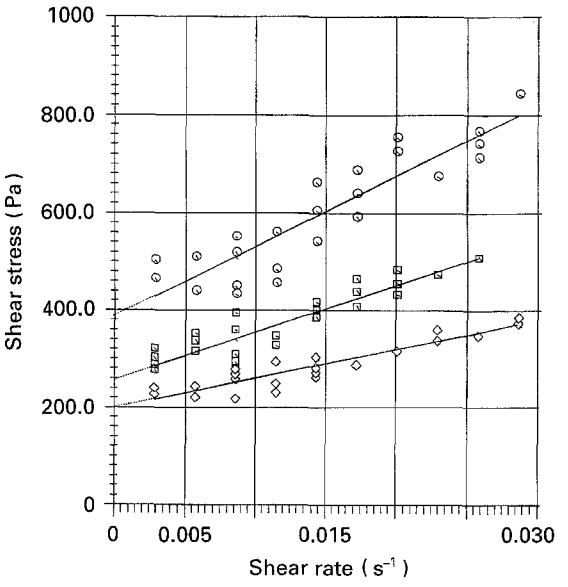

Figure 7 Method of estimation of yield stresses of feedstock No. 3 at (○) 130 (□) 150 and (◇) 170 °C. (—) Least square fitted lines.

It was found that the yield stresses obtained using the proposed method were generally lower than those obtained by direct measurement, as well as those calculated by Bingham model fit. The Casson and Herschel–Bulkley models were observed to produce relatively lower yield stress results. However, as previously discussed, these indirect methods of determining yield stress are affected by the magnitude of the shear rate range of rheological data. The yield stress values calculated from fitting of the models are dependable on the shear thinning regions of the flow data. This clearly illustrates the advantages of the proposed method over the other techniques, by overcoming the limitations of the system's resolution and the inconsistency in using mathematical models.

3.2. Wall slip

As in all practical experiments, there will be inherent experimental errors due to limitations of the method used. In rheological measurements of concentrated suspensions, the experiment is commonly affected by wall slip. Wall slip is observed and reported by investigators dealing with torsional, as well as capillary rheometry of concentrated suspensions [16, 23, 26–28, 36, 37]. The cause of wall slip is usually explained by the formation of a thin layer of a low viscosity medium at the wall. This layer is partially or completely depleted of the solid phase. Another cause could also be due to poor adhesion between the wall surface and the suspension. For torsional rheometer, it is reported that wall slips are more apparent at low shear rates, and are minimized at high shear rates. Moreover, the effects of wall slip can be reduced by using cones and plates with rough or grooved surfaces [26, 27].

Wall slip effects cause the apparent shear rates measured to be higher than the true shear rates. They would also directly cause the measured yield stress values to be lower. As the experiments are conducted using the cone and plate geometry at low shear rates, it is therefore important to check for the existence of wall slip. In papers by Magnin and Piau [26, 27] and Kalyon *et al.* [23], a flow visualization method was described to observe and measure the wall slip so as to correct the data obtained. The technique involved marking a line across the edge of the cone and plate and by using a camera and timer, wall slip can be observed and the slip velocity determined.

TABLE IV Comparison of yield stress, τ_y (Pa), values for feedstock No. 3 obtained by proposed method, direct measurement and calculation using Bingham, Casson and Herschel–Bulkley models

Temperature (°C)	Proposed method	Direct measure	Bingham model	Casson model	Herschel–Bulkley model
130	386.6	432.5	591.9	257.6	220.9
140	298.0	298.5	541.9	236.9	225.0
150	257.4	272.1	491.9	207.7	225.0
160	227.3	262.1	472.3	196.0	210.9
170	205.3	213.8	457.0	193.1	168.8
180	200.1	194.9	451.2	188.5	168.8

For experiments conducted at high temperature, the cone and plate are placed in an enclosed environment and are surrounded by an induction heating coil. The cone and plate are practically out of sight during the test. This arrangement renders the flow visualization technique to be impractical and extremely difficult to implement. As mentioned, the use of a textured or grooved surface cone and plate is believed to reduce the effects of wall slip. However, the utilization of such textured cone and plate surface might involve some sacrifice on the absolute accuracy of the rheological measurements and, moreover, the accuracy is dependent on the type of texture used.

In analysing wall slip in cone and plate rheometer using the flow visualization technique, Magnin and Piau discovered that the existence of wall slip can be determined by observing the log (shear stress) versus log (shear rate) curves. Fig. 8 illustrates such a plot.

In Fig. 8, the data for measurements with rough platen (~250 μm roughness), for which no wall slip was observed, was plotted together with that of the smooth platens for which wall slip was most significant. The behaviour of curve A demonstrates the properties of the bulk material. On the other hand, curve B shows the measurements with the smooth platens. Curve B is valid except for the decrease in stress at low shear rates that is due to slip at the wall. The higher plateau of both curves represents the properties of the bulk material. However, for curve B, the lower plateau represents the slip at the wall and is governed by the tribological conditions of the interfaces. It is solid–solid friction without viscous deformation of the bulk material. It follows that the transition from the higher to lower plateau would represent a combination of slip and material viscous flow. Although the flow visualization technique could not be implemented in the experiments, this observation by Magnin and Piau [26] serves as a check for the presence of wall slip in the yield stress measurements.

Results of the experiments indicate that feedstock Nos 2, 3 and 4 had flow curves similar to curve A (Fig. 8) indicating the absence of wall slip. The flow curves of feedstock Nos 2, 3 and 4 are shown in Fig. 9, in contrast to those of feedstock No. 1 shown in Fig. 10. However, from Fig. 10, it can be observed that a log–log scale plot of flow curves (130, 150 and 180 °C) shows a break in their slopes, exhibiting both the higher and lower plateaus. The curves are similar

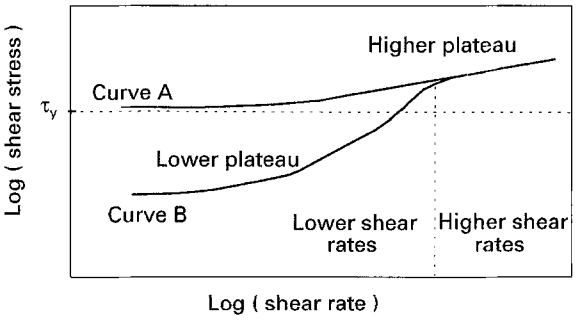

Figure 8 Generalized log (shear stress) versus log (shear rate) curves showing existence of yield stress [26].

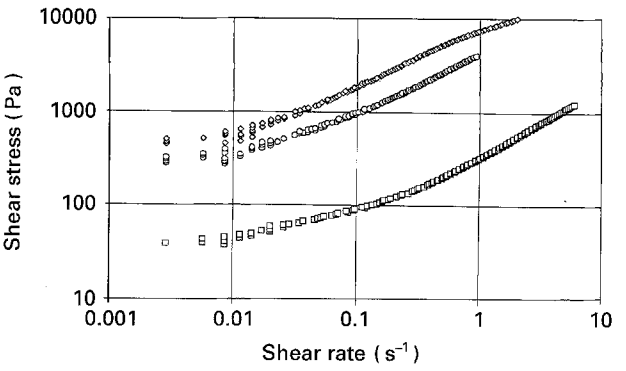

Figure 9 Log–log scale plot of flow curves for feedstocks Nos (□) 2, (○) 3 and (◇) 4, at 150 °C.

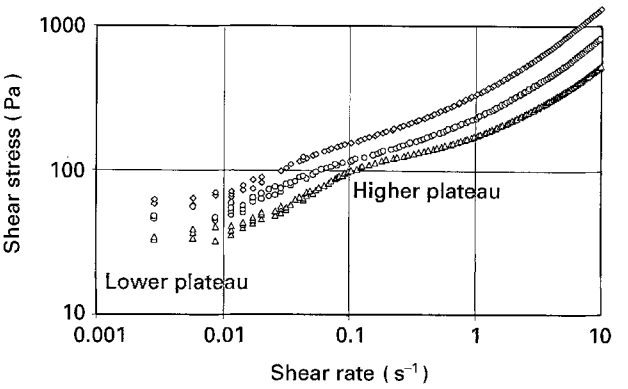

Figure 10 Log–log scale plot of flow curves for feedstocks Nos 1 at (◇) 130, (○) 150 and (△) 180 °C.

to curve B of Fig. 8 which clearly indicate the presence of wall slip during the tests with feedstock No. 1.

The cause for this observation could be due to the difference in the EVA copolymer content in the different feedstocks. Firstly, the EVA copolymer is known to have good adhesive property due to the polarity of the acetoxy groups in its molecular chains [32]. Due to the higher EVA content, feedstock Nos 2, 3 and 4 probably exhibit sufficient adhesion with the cone and plate surfaces to prevent a wall slip from occurring. However, as feedstock No. 1 contains the least amount of EVA copolymer in its binder (30 wt %), the adhesion is limited and is probably too weak to prevent a wall slip from occurring due to the shear stress at the walls of the cone and plate. Secondly, the binder of feedstock No. 1 has a relatively lower viscosity due to its higher wax to polymer ratio. It is very likely that a thin layer of low viscosity medium is formed adjacent to the cone and plate surfaces. This layer, which is partially or completely depleted of metal powders, causes the wall slip to occur. However, these explanations are still speculative at this stage. There are no tests to quantify the adhesive property, as well as the degree of phase separation in the different binder systems. Studies are in progress to examine the above phenomenon.

3.3. Effects of temperature

The yield stress of the feedstocks was determined at six different temperatures ranging from 130 to 180 °C.

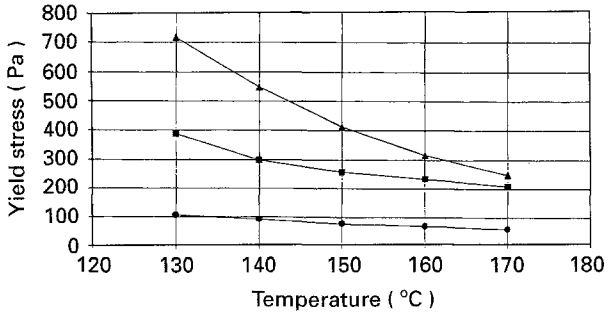

Figure 11 Yield stress versus temperature plot of MIM feedstocks: (–●–) No. 2 (40% EVA), (–■–) No. 3 (60% EVA), (–▲–) No. 4 70% EVA.

The results obtained were plotted with respect to temperature and the plot is illustrated in Fig. 11. As it was observed that wax degradation occurred at 180 °C in some of the feedstock specimens, the data for this temperature were not included in Fig. 11.

From Fig. 11, it can be observed that yield stresses of feedstocks decrease with increasing temperature. This observation contrasted with the views of Malkin [38]. In the paper [38], it was proposed that the yield stress of a filled polymer melt is independent of temperature. However, as there were neither actual experimental data nor references quoted, the proposal was difficult to verify.

At this stage, the reason for the decrease in yield stress with temperature is not understood fully. However, it was reported by Tanaka and White [39, 40], who showed the dependence of yield stress on the volume fraction of fillers in a concentrated suspension using a theoretical model approach. Experimental data were also presented to further support this dependence. It was reported that yield stress increases with increasing filler volume fraction. In the present case, the volume fraction of the feedstocks was computed based on density data at room temperature. However, due to a difference in thermal expansion coefficients of the binder and the powder, the effective solid volume fraction changes. In the event of an increase in temperature, the binder, in a liquid phase, probably expands more than the powder. This leads to a decrease in the effective solid volume fraction, which in turn causes a decrease in yield stress of the feedstock. Nevertheless, this is just one possible explanation for the decrease of yield stress with temperature.

For thermal debinding of MIM compacts, it is important for the feedstocks to have a yield stress to retain their shape. Debinding usually involves heating the compact slowly and holding at specific temperatures to remove individual components of the binder. As it was shown that yield stress decreases with increasing temperature, therefore it is advisable to heat and hold initially at a level such that the yield stress is sufficient to retain the compact's shape. Failing to do so will cause the compact to slump under its own weight and distort its shape. Evaporation of the most volatile component of the binder will take place and is allowed to occur for some time. Consequently, due to binder loss, the effective powder volume fraction in the compact is increased. The temperature can then be increased progressively to the next hold level without causing severe slumping. This process is continued until all the binder is removed. Hence, it can be seen that the yield stress plays a critical role in debinding. In view of this, parameters that influence yield stress, such as particle and binder characteristics, particle–particle interactions and binder–particle interactions, will inevitably influence the debinding schedule. The relationship between yield stress and debinding process will be investigated in detail in a future study.

The dependence of yield stress on temperature can be correlated by an Arrhenius type relationship as described by Equation 4

$$\tau_y = A \times \exp\left(\frac{E_y}{RT}\right) \quad (4)$$

where τ_y is the yield stress, A is a pre-exponential function, E_y the activation energy for yield, R is the universal gas constant (8.3144 kJ kmol^{-1} K^{-1}) and T is the absolute temperature. The activation energy for yield, E_y, gives a measure of the sensitivity of yield stress to thermal energy. A linear relationship as described by Equation 4 can be obtained by plotting log (τ_y) versus ($1/T$) as shown in Fig. 12.

To determine the activation energy for yield, E_y, the gradients of the plots were determined and multiplied by the universal gas constant, R. In comparing the E_y values, it was discovered that E_y is dependent on the EVA content in the binder. This is shown in Fig. 13. It can be observed that E_y increases with increasing EVA content. As E_y is a measure of the sensitivity of yield stress to thermal energy, this observation predicts that the effect of temperature on yield stress will be greater in feedstocks with higher EVA content.

From the above results and discussion, it can be seen that the binder formulation has an important role in the yield behaviour of the feedstock. This observation supports the notion that in a suspension, besides interparticle interactions, the interaction between the suspension medium (binder) and the particles must also be taken into account.

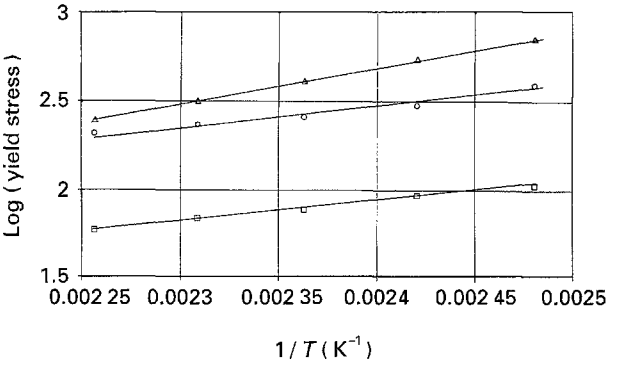

Figure 12 Plot of log (yield stress) versus ($1/T$) : (□) No. 2 (40% EVA), (○) No. 3 (60% EVA), (△) No. 4 (70% EVA).

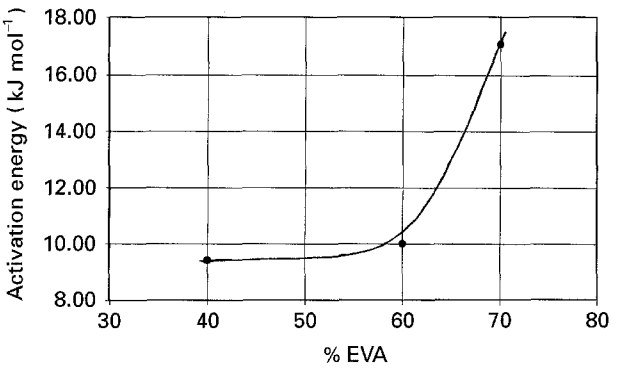

Figure 13 Variation of activation energy for yield with % EVA.

4. Conclusion

This study highlighted the difficulty in determining the yield stress of a fluid, especially at high temperatures. A method of determining yield stress was proposed based on a combination of both static and dynamic approaches, using a controlled stress rheometer fixed with a cone and plate geometry. Yield stresses of feedstocks were found to be dependent on temperature. As temperature decreased, yield stress was found to increase.

The effects of binder formulation were studied. It was found that an increase in EVA content in the binder had the following effects

1. For a given temperature, the feedstocks with higher EVA content had higher yield stresses.
2. Feedstocks with higher EVA content were found to have higher E_y, activation energy for yield.
3. The effects of temperature on yield stress were found to be greater for feedstocks with higher EVA content.

References

1. R. A. PETT, V. D. N. RAO and S. B. A. QADERI, US Patent 4158689 (1979).
2. R. D. RIVERS, US Patent 4113480 (1978).
3. R. E. WIECH Jr, US Patent 4197118 (1980).
4. *Idem*, US Patent 4415528 (1983).
5. K. P. JOHNSON, US Patent 4765950 (1988).
6. R. L. BILLIET, US Patent 4795598 (1989).
7. Y. KIYOTA, US Patent 4867943 (1989).
8. T. NAGAI, H. YAMANASHI and H. HACHIMORI, US Patent 4898902 (1990).
9. M. NAKANISHI and T. MIHO, US Patent 4968739 (1990).
10. C. A. SUNDBACK, B. E. NOVICH, A. E. KARAS and R. W. ADAMS, US Patent 5047182 (1991).
11. R. M. GERMAN, "Powder Injection Molding" (Metal Powders Industries Federation, NJ, 1990) p. 176.
12. M. J. EDIRISINGHE and J. R. G. EVANS, *J. Mater. Sci.* **22** (1987) 269.
13. R. M. GERMAN, "Powder Injection Molding" (Metal Powders Industries Federation, NJ, 1990) p. 160.
14. *Idem, ibid.* p. 158, 173, 231.
15. B.O. RHEE, PhD thesis, Renssalaer Polytechnic Institute (1992).
16. E. WINDHAB, "Proceedings of the Tenth International Congress on Rheology, Sydney", edited by P. H. T. Uhlherr (Society of Rheology, Sydney, 1988) p. 372.
17. Q. D. NGUYEN and D. V. BOGER, *Ann. Rev. Fluid Mech.* **24** (1992) 47.
18. J. P. HARNETT and R. Y. Z. HU, *J. Rheol.* **33**(4) (1989) 671.
19. D. D. KEE and C. F. CHAN MAN FONG, *J. Rheol.* **37**(4) (1993) 775.
20. D. D. KEE and C. J. DURNING, in "Polymer Rheology and Processing", edited by A. A. Collyer and L. A. Utracki (Elsevier Science Publishers, England, 1990) p. 177.
21. Q. D. NGUYEN and D. V. BOGER, *J. Rheol.* **29**(3) (1985) 335.
22. *Idem, ibid.* **27**(4) (1983) 321.
23. D. M. KALYON, P. YARAS, B. ARAL and U. YILMAZER, *ibid.* **37**(1) (1993) 35.
24. L. BOHLIN, in "Proceedings of the Tenth International Congress on Rheology, Sydney", edited by P. H. T. Uhlherr (Society of Rheology, Sydney, 1988) p. 191.
25. P. J. HANSEN and M. C. WILLIAMS, *Polym. Eng. Sci.* **27**(8) (1987) 586.
26. A. MAGNIN and J. M. PIAU, *J. Non-Newtonian Fluid Mech.* **36** (1990) 85.
27. *Idem, ibid.* **23** (1987) 91.
28. A. S. YOSHIMURA, R. K. PRUD'HOMME and H. M. PRINCEN, *J. Rheol.* **31**(8) (1987) 699.
29. E. C. BINGHAM, "Fluidity and Plasticity" (McGraw-Hill, New York, 1922).
30. W. H. HERSCHEL and R. BULKLEY, *Proc. ASTM* **26** (1926) 621.
31. W. CASSON, in "Rheology of Dispersed Systems", edited by C. C. Mill (Pergamon, London, 1959) p. 84.
32. M. HENDERSON, *IEEE Electrical Insulation Mag.* **9**(1) (1993) 30.
33. B. O. RHEE and C. I. CHUNG, "Proceedings of the Fourth APP Annual Meeting" (Metal Powders Industries Fed., NJ, 1990).
34. C. I. CHUNG, M. Y. CAO and B. O. RHEE, *ibid.*
35. "Instruction Manual for the Carri-Med CSL Controlled Stress Rheometer", edited by CarriMed Ltd, UK.
36. D. M. HUSBAND, N. AKSEL and W. GIEISSLE, *J. Rheol.* **37**(2) (1993) 215.
37. N. OHL and W. GLEISSLE, *ibid.* **37**(2) (1993) 381.
38. A. Y. MALKIN, *Adv. Polym. Sci.* **96** (1990) 70.
39. H. TANAKA and J. L. WHITE, *J. Non-Newtonian Fluid Mech.* **7** (1980) 333.
40. *Idem, Polym. Eng. Sci.* **20**(14) (1980) 949.

Received 9 May 1994
and accepted 3 February 1995